VIA MEDICA

Nuclear Medicine Review 2024, 27, 31–35
DOI: 10.5603/nmr.99794

ISSN 1506–9680, e-ISSN 1644–4345

Original

Quantitative analysis of standardized uptake values (SUV) of metastatic bone lesions in scintigraphy with [^{99m}Tc]Tc-EDDA/HYNIC-Tyr^3-octreotide in patients with neuroendocrine tumours

Marta Milena Malarz[1], Bożena Birkenfeld[2], Hanna Piwowarska-Bilska[2]

[1]Department of Nuclear Medicine, University Clinical Hospital No. 1, Pomeranian Medical University in Szczecin, Poland
[2]Department of Nuclear Medicine, Pomeranian Medical University in Szczecin, Poland

[Received 14 III 2024; Accepted 12 VI 2024]

Abstract

Background: Neuroendocrine tumours (NETs) are a group of cancers that can produce hormones and other metabolically active compounds. The majority of NETs have specific tissue characteristics, such as the expression of somatostatin receptors (SSTR). Metabolic testing with [^{99m}Tc]Tc-EDDA/HYNIC-Tyr^3-octreotide ([^{99m}Tc]Tc-EDDA/HYNIC-TOC) can be used in patients with NETs to visualise the presence of receptors in different locations of pathological lesions, including the skeletal system. The study aimed to calculate the body weight maximum standardized uptake value (SUV_{bwmax}) of pathological bone lesions and healthy bone tissues, estimate the size of lesions, and identify a relationship between the SUV_{bwmax} of the bone tissues, age and body mass of the study participants.

Material and methods: The somatostatin receptor scintigraphies (SRS) with [^{99m}Tc]Tc-EDDA/HYNIC-TOC were carried out at the Department of Nuclear Medicine, University Clinical Hospital No. 1, Pomeranian Medical University (PMU) in Szczecin from 2019 to 2022. Whole body and single photon emission computed tomography/computed tomography (SPECT/CT) scans were performed four hours after the injection of 700–800 MBq of [^{99m}Tc]Tc-EDDA/HYNIC-TOC in 344 patients with neuroendocrine tumours of various primary lesion locations. In 19 patients, who showed *foci* of increased radiopharmaceutical accumulation in bone location, the SUV_{bwmax} was measured. The SUV_{bwmax} of pathological bone lesions and healthy tissues were determined on SPECT/CT cross-sectional images using Xeleris 4 software.

Results: The total number of *foci* with increased SSTR expression in bone regions seen on scintigraphic images was 89. Among them, 32 bone lesions were visible on the corresponding CT scans. The mean SUV_{bwmax} of these lesions was 31.39 [standard deviation (SD) 34.31]. For the other 57 lesions that were not visible on corresponding CT scans, the mean SUV_{bwmax} was 19.12 (SD 24.24). The smallest bone lesion detected on the scintigram and visible on the corresponding CT location was 5 mm × 5 mm, measured in cross-section, and was located in the Th8 vertebral body; the largest, measuring 20 mm × 22 mm, was detected in the L3 vertebral body. The SUV_{bwmax} of these lesions was 24.70 and 142.40, respectively.

Conclusions: Bone lesions seen on SPECT/CT in [^{99m}Tc]Tc-EDDA/HYNIC-TOC scintigraphy can be quantitatively analysed using the SUV index. Even a very small pathological bone lesion can be detected on [^{99m}Tc]Tc-EDDA/HYNIC-TOC scintigraphy. It was shown that in cases where bone lesions were visible on CT scans, the SUV_{bwmax} of bone tumour lesions was higher than when lesions were not visible on CT. Body mass does not affect the SUV_{bwmax} of bone lesions. SUV_{bwmax} of healthy bone tissue decreased with age.

KEYwords: SUV; standardized uptake value; [^{99m}Tc]Tc-EDDA/HYNIC-TOC; NETs; neuroendocrine tumours; SSTR; SRS

Nucl Med Rev 2024; 27: 31–35

Correspondence to: Marta Milena Malarz, Department of Nuclear Medicine, University Clinical Hospital No. 1, Pomeranian Medical University in Szczecin, Unii Lubelskiej 1, 71–252 Szczecin, Poland,
e-mail: marta.malarz@usk1.szczecin.pl

Introduction

As defined by Cuthbertson et al. [1] and Juhlin and Bal [2], neuroendocrine tumours (NETs) represent a heterogeneous group of tumours, differing in their primary tumour sites, functional status (*i.e.* hormone-secreting or non-functional) and degrees of aggressiveness, ranging from grade 1 to grade 3. Neuroendocrine carcinomas (NECs) refer to separate forms of tumours that proliferate more rapidly and spread more quickly. The most common primary sites are the lung, small bowel, pancreas and appendix.

In Poland, NETs account for about 2% of all malignancies, and their incidence steadily rises. Due to the broad spectrum of malignancy and the variety and non-specificity of symptoms, the diagnosis of neuroendocrine tumours is often made at an advanced stage [3]. The diagnosis is based on the patient clinical picture, blood biomarker evaluation, and imaging modalities like CT, MR and scintigraphy [1]. The majority of NETs have specific tissue characteristics, including the expression of somatostatin receptors (SSTRs), the presence of which can be demonstrated by somatostatin receptor scintigraphy (SRS). Patients with NETs can be imaged with single photon emission computed tomography/computed tomography (SPECT/CT), which allows for obtaining precise information about the location of the lesions in the skeletal system. A possible alternative to [^{99m}Tc]Tc-EDDA/HYNIC-TOC examination is [^{68}Ga]Ga-DOTA-TATE, which requires the ^{68}Ge/^{68}Ga generator and PET/CT modality [4], making this procedure quite expensive and not widely available.

Testing for SSTRs has become an integral part of diagnostics in nuclear medicine over the past 20 years, beginning with the launch of [^{111}In-DTPA-DPhe^{1}]-octreotide [5]. The radioisotope-labelled somatostatin scintigraphy helps diagnose NETs and is crucial in deciding on treatment with not labelled or radio-labelled somatostatin analogues for unresectable metastatic neuroendocrine tumours [6, 7]. The analysis of SRSs is done mostly quantitatively. Qualitative analysis is possible with modern gamma cameras and software, calculating the SUV of pathological lesions.

A large group of patients with NETs underwent SRSs in the Department of Nuclear Medicine, University Clinical Hospital No. 1, Pomeranian Medical University (PMU) in Szczecin. For the body weight maximum standardized uptake value (SUV_{bwmax}) analysis were selected patients with metastatic lesions in the skeletal system detected in SPECT/CT scintigraphy with [^{99m}Tc]Tc-EDDA/HYNIC-TOC, considering that in this group it was possible to measure the lesions using the CT part of hybrid imaging. The study aimed to calculate the SUV_{bwmax} of pathological bone lesions and healthy bone tissues, estimate the size of lesions, and identify a relationship between the SUV_{bwmax} of the bone tissues, age and body mass of the study participants.

Material and methods

SRSs with [^{99m}Tc]Tc-EDDA/HYNIC-TOC were performed at the Department of Nuclear Medicine of in 344 patients (196 women and 148 men) with NETs of various locations between 2019 and 2022. Whole body and SPECT/CT imaging tests were performed in all patients four hours after radiopharmaceutical intravenous injection with an activity of approximately 800 MBq. The authors conducted a retrospective analysis of scans and screened them for tracer accumulation in bone lesions. Identified were 89 lesions of increased expression of SSTR in different parts of the skeleton in 19 out of 344 patients, 12 males and 7 females aged 31–80 years. In 4 patients, the primary tumours were located in the lungs, in 1 patient — in the adnexis, and in 14 they were located in the gastrointestinal tract. Patients were imaged using the NM/CT850 GE Healthcare gamma camera. The scintigraphies were evaluated by two independent doctors. The SUV_{bwmax} of bone lesions was determined on SPECT cross-sectional images of patients using Xeleris 4 software. The SUV_{bw} was calculated using the following formula [8]:

$$SUV_{bw} = \frac{\text{SPECT image Pixels uptake (Bq/mL)} \times \text{weight (g)}}{\text{(actual activity)}} \quad (1)$$

where:

actual activity: activity during scanning,

$$\text{pixels uptake (Bq/mL)} = 37 \times 10^3 \times \frac{60}{\text{SPECT sensitivity (counts/min/}\mu\text{Ci)} \times \text{T (s)} \times \text{mL}} \quad (2)$$

where T — scan duration in seconds.

The transverse and longitudinal sizes of the visible bone lesion were measured on CT image slices. The method of segmentation and measuring the size of the bone lesion is shown in Figure 1.

Statistical analysis was used to answer the research questions. Descriptive statistics together with Shapiro–Wilk tests were performed for the dependent variables. Spearman's *rho* correlation

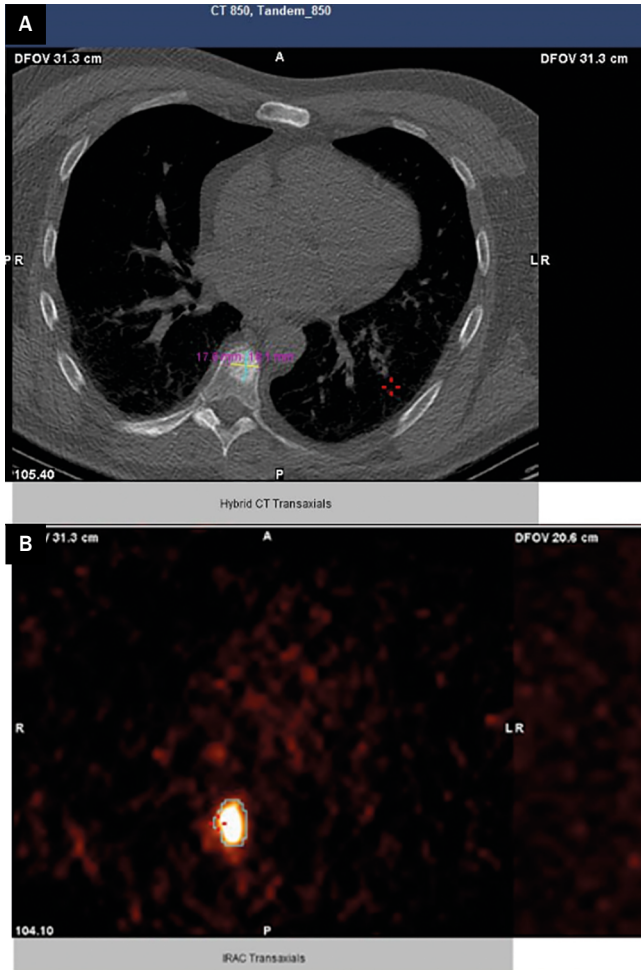

Figure 1. On the axial CT cross-section (**A**) and the corresponding SPECT axial cross-section (**B**) a pathological lesion is visible in the vertebral body of vTh6

Table 1. Patients and pathological bone lesions data

Dependent variable	Mean	Median	SD	Min	Max	p-value
Age [years]	58.53	64.00	14.57	31.00	80.00	< 0.001
Body weight [kg]	70.97	73.00	11.30	55.00	90.00	0.003
Transverse dimension of the bone lesion [mm]	10.41	9.00	4.84	3.00	20.00	0.091
Longitudinal dimension of the bone lesion [mm]	12.42	11.50	5.14	5.00	23.00	0.162
SUV_{bwmax}	23.53	13.72	28.70	1.02	142.40	< 0.001
Background SUV_{bwmax}	2.54	1.43	2.08	0.35	6.60	< 0.001

Min — minimum; Max — maximum; SD — standard deviation, SUV_{bwmax} — body weight maximum standardized uptake value

Table 2. Comparison of SUV_{bwmax} of malignant bone lesions and healthy bone tissue (background)

	SUV_{bwmax}		Background SUV_{bwmax}				
Dependent variable	M	SD	M	SD	z-score	p-value	r-value
SUV_{bwmax}	23.53	28.70	2.54	2.08	−7.67	< 0.001	0.61

M — mean; SD — standard deviation; SUV_{bwmax} — standardized uptake value

Table 3. Spearman's *rho* correlation analysis of SUV_{bwmax} in healthy bone lesions with age and body mass

Variable		Age	Body weight
SUV_{bwmax}	Spearman's *rho*	–	0.16
	Significance	–	0.133
Background SUV_{bwmax} (in L5 vertebral bodies)	Spearman's *rho*	−0.41	0.04
	Significance	< 0.001	0.696

SUV_{bwmax} — standardized uptake value

and Mann–Whitney U and Wilcoxon tests were performed. The significance level was set at $\alpha = 0.05$.

Results

The SSTR SPECT/CT scintigraphy with [^{99m}Tc]Tc-EDDA/HYNIC-TOC detected 89 metastatic bone lesions in 19 patients. There were 32 pathological lesions visible on SPECT and measurable on CT hybrid scanning, and 57 lesions seen on SPECT but not on CT — there was no altered bone morphology on CT in the corresponding area. The smallest bone lesion seen on SPECT/CT was 5 mm × 5 mm in size and the largest was 20 mm × 22 mm. The range of SUV_{bwmax} of all observed bone lesions was 1.02–142.40; the median SUV_{bwmax} of all lesions was 13.72. The SUV_{bwmax} of the smallest lesion, located in vTh8, was 24.70, and the SUV_{bwmax} of the largest lesion, located in vL3, was 142.40. SUV_{bwmax} of all lesions were compared with SUV_{bwmax} of bone areas with normal uptake and morphologically normal tissue observed on CT scan. The regions of interest were located in vL5 vertebral bodies (background).

Descriptive statistics and Shapiro–Wilk tests were used to examine possible deviations from normality of dependent variables (Tab. 1).

Shapiro–Wilk tests were significant for four of the seven variables, suggesting a deviation from normal distribution. Non-parametric analyses were used to verify the examined relationships between variables. An analysis of SUV_{bwmax} differences between malignant bone lesions and healthy bone tissues (background) in the study group was performed with the Wilcoxon test and the results are presented in Table 2.

The analysis revealed that the SUV_{bwmax} of malignant bone lesions was significantly higher than that of healthy bone tissues. The coefficient value r indicates a large magnitude of these differences. The relationship between SUV_{bwmax} of bone tumour lesions and the age and body mass of the study participants was tested for correlations using Spearman's *rho*. The results are presented in Table 3. The analysis revealed that SUV_{bwmax} of healthy bone tissue decreased with age. No correlation was found between body mass and SUV_{bwmax}. The analysis revealed that in the cases where lesions were visible on CT scans, the SUV_{bwmax} of the bone tumour lesions was higher than when the lesions were not visible on CT (Tab. 4).

Discussion

Calculating SUVs is a relatively new method of analysing SPECT/CT images. Quantitative analysis of lesions in scintigraphic images using the SUV index has been used mainly in PET/CT [9]. Only in recent years have there been publications on the standardisation and harmonisation of methods for calculating SUV in SPECT/CT [10, 11]. The SUV_{bwmax} index became an osteoblastic biomarker in SPECT/CT scintigraphy when iterative image reconstruction opened the way to absolute quantification of SPECT/CT scans by incorporating attenuation and scatter compensation,

Table 4. Comparison of SUV_{bwmax} in bone tumour lesions between visible and non-visible lesions on CT

Dependent variable		Lesion not visible on CT (n = 57)	Lesion visible on CT (n = 32)	z-score	p-value
SUV_{bwmax}	M	19.12	31.39	−2.87	0.004
	Md	10.20	18.75		
	SD	24.24	34.31		
	Mean rank	39.11	55.48		
Background SUV_{bwmax} (in L5 vertebral bodies)	M	2.36	2.94	−0.03	0.974
	Md	1.43	1.06		
	SD	1.63	2.82		
	Mean rank	39.56	39.38		

M — mean; Md — median; SD — standard deviation; SUV_{bwmax} — standardized uptake value

as well as detector resolution correction, into the reconstruction process [12]. Nevertheless, optimising and standardising the technique of determining SUV indices in SPECT/CT remains a challenge for nuclear medicine [13]. When comparing the obtained SUVs, it is important to remember that the index is affected by several technical factors, such as the result of the camera range calibration, image reconstruction method and the segmentation method for areas of interest.

The present study performed a quantitative analysis of the SUV_{bwmax} of metastatic bone lesions in patients with neuroendocrine tumours on SPECT/CT after intravenous administration of [^{99m}Tc]Tc-EDDA/HYNIC-TOC. The statistical analysis of these index values has shown that lesions visible on CT scans showed higher SUV_{bwmax} than lesions that did not alter the morphological structure of the bone. Interestingly, despite the lack of bone morphologic structure lesions, the changes were not visible on CT scans; the SPECT showed focal increased tracer accumulation in the bone. It can be assumed that bone morphology will undergo remodelling due to metastatic background, and the pathological lesion may become visible on CT scans after some time. This information is clinically important as it confirms the high profile of metabolic testing and its high sensitivity. False positive results of increased receptor expression can be observed in the cases of inflammatory changes in various organs, degenerative bone changes, and growth cartilage in juveniles [14]. In patients with NETs, SRS can reveal areas of increased [^{99m}Tc]Tc-EDDA/HYNIC-TOC accumulation of a metastatic nature in the bone marrow [15]. These changes may be related to elevated receptor expression in the bone marrow, which has not been reflected in the CT imaging of the bones in the studied group of patients.

In the present study, the smallest lesion that showed increased expression of somatostatin receptors was 5 mm × 5 mm in transverse and longitudinal sections. Out of 89 lesions, 57 showed increased expression of SSTR and were not visible in CT — there was no change in the morphological structure of the bones. Briganti et al. [4] presented a study in which they showed that [^{68}Ga]Ga-DOTA-TATE PET is the best choice as it guarantees a minimum spatial resolution threshold of 4–5 mm, and 7–9 mm for [^{99m}Tc]Tc-EDDA/HYNIC-TOC. However, the present study has shown that using the [^{99m}Tc]Tc-EDDA/HYNIC-TOC is also justified in diagnosing metastatic neuroendocrine tumours, as it can detect lesions as small as 5 mm. Moreover, in cases where skeletal changes were not visible on CT, increased radiopharmaceutical accumulation was observed in SPECT, indicating that even smaller lesions can be detected. However, the presence of SSTR is a crucial factor.

Trogrlic and Tezak [16], who in 2016, studied 16 patients with neuroendocrine tumours of the head and neck, with a mean age of 57.7 note that bone was the most common location of distant metastases in 5 out of 16 patients (31%). In the present study, bone lesions were detected on the images of 19 (6%) out of 344 patients examined and the mean SUV_{bwmax} of bone lesions was 23.53 (SD 28.70). In their study conducted in 2021, Reilly et al. [17] examined [^{99m}Tc]Tc-EDDA/HYNIC-TOC uptake in patients with neuroendocrine tumours in the liver, spleen, kidneys and bones, as well as in locations affected by the underlying disease. SUV_{bwmax} of bone metastases was 12.9 on average. Significant differences were observed between normal and metastatic SUVs in the liver and bone. In a 2023 paper, Gherghe et al. [18] showed that out of 14 patients studied, bone lesions were observed in three patients, who had a mean SUV_{bwmax} of 5.90.

The method of calculating SUV index by SPECT/CT is a relatively new technique that certainly needs to be clarified and standardised particularly given that the [^{99m}Tc]Tc-EDDA/HYNIC-TOC is used for the diagnostics of patients with NETs in only a few countries, mainly in Europe. The number of publications on the presented topic remains small, however, due to the increasing prominence of nuclear medicine in diagnostics and especially the tendency and need for quantitative analysis, the authors hope that this research sheds some new light on this subject. It was shown that SUV calculation is a valuable method for somatostatin receptor scintigraphy analysis.

Conclusions

1. In cases where bone lesions were visible on CT scans, the SUV_{bwmax} of bone tumour lesions was higher than when the lesions were not visible on CT.
2. Even a small metastatic bone lesion can be detected on SPECT/CT scintigraphy with [^{99m}Tc]Tc-EDDA/HYNIC-TOC.
3. The SUV_{bwmax} of healthy bone tissue decreases with age.
4. Body mass had no effect on the SUV_{bwmax} of normal bone lesions for the study group of patients with NETs.

Article information and declarations

Acknowledgements

None.

Author contributions

All authors contributed to the study's conception and design. Material preparation, data collection and analysis were performed — MM, BB, and HPB. The first draft of the manuscript — MM. All authors commented on previous versions of the manuscript. All authors read and approved the final manuscript.

Funding

None.

Data availability statement

Test results are stored at the Department of Nuclear Medicine, University Clinical Hospital No. 1 PMU, Szczecin, Poland. For any questions, please contact the corresponding author.

Ethics statement

Patients gave written consent for their results to be used in the research paper.

Conflicts of interest

The authors declare that they have no competing interests.

Supplementary material

None.

References

1. Cuthbertson DJ, Shankland R, Srirajaskanthan R. Diagnosis and management of neuroendocrine tumours. Clin Med (Lond). 2023; 23(2): 119–124, doi: 10.7861/clinmed.2023-0044, indexed in Pubmed: 36958842.
2. Juhlin CC, Bal M. Top 10 histological mimics of neuroendocrine carcinoma you should not miss in the head and neck. Head Neck Pathol. 2023; 17(1): 66–84, doi: 10.1007/s12105-022-01521-x, indexed in Pubmed: 36941503.
3. Kos-Kudła B, Bartmańska M. Wczesne rozpoznawanie nowotworów neuroendokrynnych w Polsce – wyniki kwestionariusza medycznego [Early diagnosis of neuroendocrine tumors in Poland - results of a medical questionnaire]. Pol Merkur Lekarski. 2022; 50(300): 364–369, indexed in Pubmed: 36645682.
4. Briganti V, Cuccurullo V, Berti V, et al. Tc-EDDA/HYNIC-TOC is a new opportunity in neuroendocrine tumors of the lung (and in other malignant and benign pulmonary diseases). Curr Radiopharm. 2020; 13(3): 166–176, doi: 10.2174/1874471013666191230143610, indexed in Pubmed: 31886756.
5. Mikołajczak R, Maecke HR. Radiopharmaceuticals for somatostatin receptor imaging. Nucl Med Rev Cent East Eur. 2016; 19(2): 126–132, doi: 10.5603/NMR.2016.0024, indexed in Pubmed: 27479790.
6. Putzer D, Gabriel M, Henninger B, et al. Bone metastases in patients with neuroendocrine tumor: 68Ga-DOTA-Tyr3-octreotide PET in comparison to CT and bone scintigraphy. J Nucl Med. 2009; 50(8): 1214–1221, doi: 10.2967/jnumed.108.060236, indexed in Pubmed: 9617343.
7. Kwekkeboom D, Krenning E, de Jong M. Peptide receptor imaging and therapy. J Nucl Med. 2000; 41(10): 1704–1713, indexed in Pubmed: 11038002.
8. NM Quantification. Q.Metrix for SPECT/CT Package. White Paper, DOC1951185, 2017, GE Healthcare.
9. Sharma P, Chatterjee P, Alvarado LA, et al. Standardized uptake value of normal organs on routine clinical [18F]FDG PET/CT: impact of tumor metabolism and patient-related factors. Nucl Med Rev Cent East Eur. 2023; 26(0): 1–10, doi: 10.5603/NMR.a2022.0036, indexed in Pubmed: 36286203.
10. Halim F, Yahya H, Jaafar KN, et al. Accuracy assessment of SUV measurements in SPECT/CT: a phantom study. J Nucl Med Technol. 2021; 49(3): 250–255, doi: 10.2967/jnmt.120.259168, indexed in Pubmed: 33722927.
11. Dickson JC, Armstrong IS, Gabiña PM, et al. EANM practice guideline for quantitative SPECT-CT. Eur J Nucl Med Mol Imaging. 2023; 50(4): 980–995, doi: 10.1007/s00259-022-06028-9, indexed in Pubmed: 36469107.
12. Peters SMB, van der Werf NR, Segbers M, et al. Towards standardization of absolute SPECT/CT quantification: a multi-center and multi-vendor phantom study. EJNMMI Phys. 2019; 6(1): 29, doi: 10.1186/s40658-019-0268-5, indexed in Pubmed: 31879813.
13. Piwowarska-Bilska H, Kurkowska S, Birkenfeld B. Optimized method for normal range estimation of standardized uptake values (SUVmax, SUVmean) in liver SPECT/CT images with somatostatin analog [99mTc]-HYNIC-TOC (Tektrotyd). Nucl Med Rev Cent East Eur. 2022; 25(1): 37–46, doi: 10.5603/NMR.a2022.0008, indexed in Pubmed: 35137936.
14. Garai I, Barna S, Nagy G, et al. Limitations and pitfalls of 99mTc-EDDA/HYNIC-TOC (Tektrotyd) scintigraphy. Nucl Med Rev Cent East Eur. 2016; 19(2): 93–98, doi: 10.5603/NMR.2016.0019, indexed in Pubmed: 27479887.
15. Basu S, Ranade R, Thapa P. Metastatic neuroendocrine tumor with extensive bone marrow involvement at diagnosis: evaluation of response and hematological toxicity profile of PRRT with (177)lu-dotatate. World J Nucl Med. 2016; 15(1): 38–43, doi: 10.4103/1450-1147.165353, indexed in Pubmed: 26912977.
16. Trogrlic M, Tezak S. 99mTc-EDDA/HYNIC-TOC in management of patients with head and neck somatostatin receptor positive tumors. Nucl Med Rev Cent East Eur. 2016; 19(2): 74–80, doi: 10.5603/NMR.2016.0016, indexed in Pubmed: 27479884.
17. Reilly C, Gemmell AJ, McLaughlin IM, et al. Characterisation of 99mTc EDDA/HYNIC-TOC (Tektrotyd) physiological and neuroendocrine tumour uptake using SPECT/CT standardised uptake values: initial experience. Nucl Med Commun. 2021; 42(8): 935–939, doi: 10.1097/MNM.0000000000001416, indexed in Pubmed: 33741866.
18. Gherghe M, Lazar AM, Simion L, et al. Standardized uptake values on SPECT/CT: a promising alternative tool for treatment evaluation and prognosis of metastatic neuroendocrine tumours. Diagnostics (Basel). 2023; 13(2): 318, doi: 10.3390/diagnostics13020318, indexed in Pubmed: 36673128.